Journal of Nanoparticle Research (2007) 9:1027–1039
DOI 10.1007/s11051-006-9183-5


*Research Paper*

# Zinc sulfide nanoparticles: Spectral properties and photocatalytic activity in metals reduction reactions

A. L. Stroyuk, A. E. Raevskaya, A. V. Korzhak and S. Y. Kuchmii
*Photochemistry department, Pisarzhevski Institute of Physical Chemistry, National Academy of Sciences of Ukraine, 31 Nauky av., 03028, Kiev, Ukraine; *Author for correspondence (Tel.: +38-044-5250270; E-mail: stroyuk@inphyschem-nas.kiev.ua)*

Received 15 November 2005; accepted in revised form 22 September 2006

*Key words:* ZnS nanoparticles, quantum confinement, semiconductor photocatalysis, metal-semiconductor nanocomposites, zinc reduction, gold nanoparticles, plasmon resonance

## Abstract

Formation of zinc sulfide nanocrystals in aqueous solutions of various polymers has been studied. Spectral properties of ZnS nanoparticles have been investigated, the structure of the long-wave edge of the fundamental absorption band of ZnS nanocrystals has been analyzed. It has been shown that the variation of the synthesis conditions (stabilizer nature and concentration, solution viscosity, ZnS concentration, etc.) allows tailoring of the ZnS nanocrystals size in the range of 3–10 nm. Photochemical processes in colloidal ZnS solutions, containing zinc chloride and sodium sulfite, have been investigated. It has been found that the irradiation of such solutions results in the reduction of Zn(II), the rate of this reaction growing at a decrease in the size of ZnS nanoparticles. Kinetics of photocatalytic Zn(II) reduction has been studied. It has been concluded that two-electron reduction of adsorbed Zn(II) species is the rate-determining stage of this reaction. Photocatalytic activity of ZnS nanoparticles in $KAu(CN)_2$ reduction in aqueous solutions has been discovered. Spectral characteristics and kinetics of $ZnS/Au^0$ nanocomposite formation have been studied. It has been shown that the photoreduction of gold(I) complex is the equilibrium reaction due to the reverse oxidation of gold nanoparticles by ZnS valence band holes.

## Introduction

Among the semiconductors with photochemical activity, a group of universal photocatalysts may be distinguished, which are active in a variety of photoreactions – $TiO_2$, CdS, ZnO and ZnS (Grätzel, 1983). Zinc sulfide can be distinguished in this group due to comparatively high potentials of conduction band (CB) electrons and valence band (VB) holes ($E_{CB} = -1.75$ V, $E_{VB} = +1.85$ V *versus* normal hydrogen electrode (NHE)) (Kanemoto et al., 1996), favorable for photocatalytic transformation of a wide range of substrates.

It is known that a decrease of the size of semiconductor nanoparticles ($2R$) down to the values, comparable with the delocalization domain of photogenerated exciton, $2a_B$, (where $a_B$ is a Bohr exciton radius, equal for ZnS to 3.0 nm (van Dijken et al., 1998)) quantum size effects can be observed, consisting in a growth of the band gap $E_g$ and the energies of the allowed bands $E_{CB}$ and $E_{VB}$, inversely proportional to $R^2$ (Wang & Herron,

1991; Gaponenko, 1996). Quantum-confined zinc sulfide nanoparticles proved to have advanced, as compared to bulk (micrometer) ZnS crystals, photocatalytic activity in many redox-processes. In some cases, ZnS nanocrystals can even participate in the reactions, thermodynamically prohibited for bulk zinc sulfide (Kanemoto et al., 1992, 1996). So, utilization of ZnS nanocrystals with quantum size effects opens new route to the intensification of photocatalytic processes (Kanemoto et al., 1992; Yanagida et al, 1990), as well as the control of the dynamics of the photocatalytic reactions through variation of ZnS nanocrystals size (Yanagida et al., 1989, 1990).

At the same time, many aspects of the chemistry and photochemistry of ZnS nanocrystals remain still unexplored. Among them are the effect of synthesis conditions on the size, optical and photochemical properties of ZnS nanoparticles, their photocatalytic activity in metals deposition, properties of ZnS-based metal-semiconductor nanostructures, etc.

Photocatalytic metals deposition onto the surface of semiconductor nanocrystals is one of the most convenient methods of the preparation of metal-semiconductor nanocomposites with advanced photochemical activity. This method has been applied to synthesize nanostructured photocatalysts for the reduction of water (CdS/Ni (Stroyuk et al., 2004), $TiO_2$/Ni (Korzhak et al., 2005)), metal ions (ZnO/Ag (Stroyuk et al., 2005)), ketones (CdS/Cd (Shiragami et al., 1992)), aromatic nitrocompounds ($TiO_2$/Ag (Tada et al., 2005)), etc. One may therefore expect that the modification of the surface of ZnS nanocrystals with metal nanoclusters, which are capable to accumulate the photogenerated charge carriers and accelerate reductive redox-reactions, will result in an enhancement of the efficiency of the photoprocesses with the participation of ZnS nanoparticles.

The choice of the objects of the present paper has been determined by the circle of above-discussed problems. In the first part of the paper we discuss the effect of the synthesis conditions upon the size and spectral characteristics of aqueous colloidal ZnS solutions. Photocatalytic activity of ZnS nanocrystals in Zn(II) reduction by sodium sulfite in aqueous solutions is discussed in the second part of the paper. Finally, the third section of the paper is devoted to the duscission of the photocatalytic activity ZnS nanoparticles in $KAu(CN)_2$ complex reduction as well as the analysis of the spectral properties of ZnS/Au nanostructures, formed in the course of this reaction.

## Experimental

Reagent grade chemicals have been used in all experiments. Zinc sulfide nanoparticles have been prepared via the interaction between $Zn(CH_2COO)_2$ and $Na_2S$ in aqueous stabilizer solutions. Sodium polyphosphate (SPPh), polyvinyl alcohol (PVA), photographic gelatine, sodium docecyl sulfate (SDS), cetylpyridinium chloride (CPC) or an excess of zinc acetate has been used as a stabilizer. In some experiments, ZnS nanocrystals have been synthesized in water–glycerol mixtures. SPPh has been used as the stabilizer of colloidal solutions at the investigation of photocatalytic properties of ZnS nanoparticles.

Reaction mixtures have been prepared via the addition of an aliquot of the stock $Na_2SO_3$ (1.0 M), $Zn(CH_3COO)_2$ (0.1 M) and $KAu(CN)_2$ (0.1 M) solutions to ZnS colloid, stabilized with SPPh. Concentrations of the components have been varied in the following range: $[Na_2SO_3] = 5{\cdot}10^{-3}-2{\cdot}10^{-2}$ M, $[Zn(CH_3COO)_2] = 5{\cdot}10^{-4}-5{\cdot}10^{-3}$ M, $[ZnS] = 5{\cdot}10^{-4}-5{\cdot}10^{-3}$ M, $[SPPh] = 5{\cdot}10^{-4}-1{\cdot}10^{-2}$ M.

Irradiation has been carried out in quartz parallel-sided optical 10.0 mm cuvettes with 254 nm light source. Maximal light intensity used was $I_0 = 1{\cdot}10^{-6}$ Einstein$\cdot$ min$^{-1}$. In some experiments solutions have been degassed via continuous argon bubbling.

Absorption spectra have been registered on the Specord M40 double-beam spectrophotometer. Absorption coefficients of colloidal ZnS solutions ($\alpha$, cm$^{-1}$) have been calculated using the expression $\alpha = 2303{\cdot}\, D{\cdot}\, \rho{\cdot}C^{-1}{\cdot}\, l^{-1}$ (Gaponenko, 1996), where $D$ is the optical density of a solution, $\rho$ is the density of bulk ZnS crystals (4.087 g$\cdot$cm$^{-3}$), C is the ZnS concentration (g$\cdot$cm$^{-3}$) $l$ is the optical path (cm).

The average sizes of ZnS nanoparticles have been estimated in the approximation of the effective masses of charge carriers (Wang & Herron, 1991; Gaponenko, 1996) using expression (1):

$$\Delta E_g = \frac{-\hbar^2\pi^2}{2R^2}\left(\frac{1}{m_e^* m_0} + \frac{1}{m_h^* m_0}\right) \quad (1)$$

where $\Delta E_g$ is the odds between the $E_g$ values of nanometer and bulk ZnS crystals (for bulk cubic

zinc sulfide $E_g^{bulk} = 3.6$ eV (Yanagida et al., 1990; van Dijken, 1999)), $\hbar$ is the reduced Planck constant, $m_e^* = 0.34m_0$, $m_h^* = 0.5\ m_0$ (van Dijken et al., 1998)) are the effective masses of conduction band electron and valence band hole respectively, $m_0$ is the electron rest mass.

The values of $E_{CB}$ and $E_{VB}$ of ZnS nanocrystals have been determined using the following expressions (Kryukov et al., 2000):

$$E_{CB} = E_{CB}^{bulk} - \Delta E_g \cdot m_h^* \cdot (m_e^* + m_h^*)^{-1},$$

$$E_{VB} = E_{VB}^{bulk} + \Delta E_g^* e \cdot (m_e^* + m_h^*)^{-1},$$

X-rays diffraction (XRD) spectra have been registered using DRON-3M diffractometer, operating with copper $\kappa_\alpha$-line irradiation.

## Results and discussion

### *Spectral properties of ZnS nanoparticles*

Colloidal SPPh-stabilized zinc sulfide solution is stable toward aggregation at molar concentrations [ZnS] $< 1 \cdot 10^{-2}$ M, but it coagulates quickly at higher ZnS content. There are three strongly widened peaks at $2\theta = 25.6$, 45.6 and $55.3^0$ in XRD spectra of the coagulates (Figure 1), corresponding to cubic zinc blende modification of zinc sulfide (van Dijken et al., 1998; Dhas et al., 1999; Nanda et al., 2000; Zhang et al., 2003). Estimations based on Scherer equation (van Dijken et al., 1998; Nanda et al., 2000; Zhang et al., 2003) and the FWHMs of the peaks in XRD spectra have shown that coagulates of ZnS colloids consist of

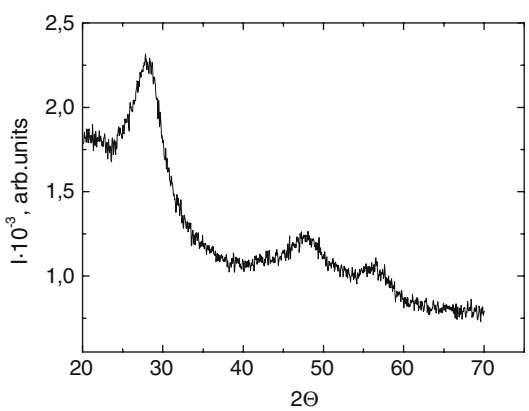


*Figure 1.* XRD spectrum of ZnS nanocrystals.

7.0–7.5 nm crystals. So, we can conclude that colloidal ZnS solutions, which are stable toward the coagulation, consist of smaller crystals, i.e., the solutions with [ZnS] $< 1 \cdot 10^{-2}$ M contain ZnS nanocrystals, smaller than 7.0 nm.

Position of the long-wave edge of the absorption band ($\lambda_{tr}$) in electronic spectra of ZnS colloids depends on the preparation conditions (Figure 2a) and varies from 290 to 340 nm (see Table 1). Bulk cubic crystals of zinc sulfide have $E_g^{bulk} = 3.6$ eV and the corresponding absorption threshold at $\lambda_{tr}^{bulk} = 345$ nm. Hypsochromic shift of the $\lambda_{tr}$ position of colloidal ZnS nanoparticles relatively to $\lambda_{tr}^{bulk}$ is one of the consequences of space exciton confinement in ZnS nanocrystals.

### *Assignment of electronic transitions in ZnS nanocrystals*

Generalized spectral dependence $\alpha$ ($\lambda$) for semiconductors is given by the following expression (Ramsden & Grätzel, 1984):

$$\alpha = A\frac{(h\nu - E_g)^n}{h\nu} \tag{2}$$

where $A$ is a coefficient, determined by the probability of the given electronic transition, whereas $n$ depends on the type of the transition. It is equal to $^1/_2$ and 2 in cases of allowed direct and indirect transitions, $^3/_2$ and 3 – in case of forbidden direct and indirect transitions respectively. Function (3) – derivative of the expression (2) – has a break point at $h\nu = E_g$ (Figure 2b). Using this function we can precisely determine the value of $E_g$.

$$\frac{d\{\ln(\alpha \cdot h\nu)\}}{d(h\nu)} = \frac{n}{h\nu - E_g} \tag{3}$$

Band gaps of colloidal ZnS solutions, synthesized in various conditions, as well as the average radii of ZnS nanoparticles, calculated from $E_g$ using the Eq. (1) are summarized in Table 1.

Long-wave slopes of the absorption spectra of ZnS nanoparticles (Figure 2a) have been found to be linear in the coordinates $\ln(\alpha \cdot h\nu) - \ln(h\nu - E_g)$ (Figure 2c). The slope ratio of the linear anamorphosis from the Figure 2c, corresponding to $n$ in the Eq. (2), is equal to $0.50 \pm 0.02$. Hence, long-wave light absorption of ZnS nanocrystals originates from the allowed direct interband electronic transitions.

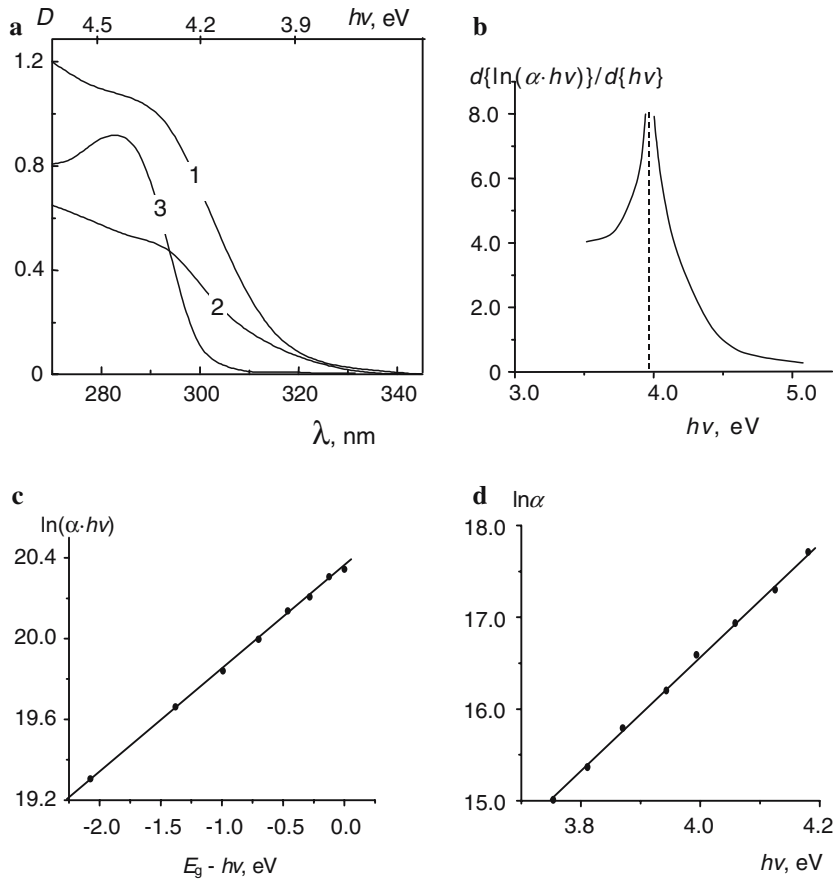


*Figure 2.* (a) Absorption spectra of colloidal ZnS solutions in water (1, 2) and glycerol (3). [ZnS] = $1 \cdot 10^{-3}$ (1, 2) and $2 \cdot 10^{-3}$ M (3). Solution (1) is stabilized with SPF ($5 \cdot 10^{-3}$ M), solution (2) is not stabilized, solution (3) is stabilized with Zn(II) ([Zn(II)] = $1 \cdot 10^{-3}$ M). Cuvette thickness $d$ = 1.0 (1), 0.5 (2) and 0.2 cm (3). (b) Anamorphosis of the spectral curve 1 (Figure 2a) in the coordinates $d\{\ln(\alpha \cdot h\nu)\}/d\{h\nu\}$–$h\nu$. Dashed line corresponds to the breaking point of the function (c) Anamorphosis of the curve 1 (Figure 2a) in the coordinates $\ln(\alpha \cdot h\nu)$–$(E_g - h\nu)$. (d) Anamorphosis of the spectral curve 3 (Figure 2a) in the coordinates $\ln\alpha$–$h\nu$

It can be seen from the spectral curves, presented on the Figure 2a, that ZnS nanoparticles can absorb light quanta with energy $h\nu$, smaller than $E_g$. Light absorption at $h\nu < E_g$ may be associated with wide size distribution of ZnS nanoparticles (in this case, light with $h\nu < E_g$ is absorbed by the fraction of larger ZnS nanocrystals) or with high defects concentration in the lattice of ZnS nanocrystals. These defects lay under the edge of the conduction band and are capable to ionize, absorbing light with $h\nu < E_g$. Analysis of the spectral curve 3 from the Figure 2a let us derive two arguments in favor to the second assumption. First, the distinct maximum, corresponding to the first excitonic transition in ZnS nanocrystals, can be seen on the spectral curve 3. It is known, that sharp excitonic maxima are observed only in case of monodisperse colloidal semiconductors (Wang & Herron, 1991; Dhas et al., 1999; Nanda et al., 2000). Second, a section of the curve 3, satisfying the condition $h\nu < E_g$ (i.e., $\lambda > 300$ nm) appears to be linear in the coordinates of Uhrbach Eq. (4), giving the correlation between the defect absorbance and the excitatory quanta energy (Figure 2e) (Ramsden & Grätzel, 1984).

*Table 1.* Absorption band edge ($\lambda_{tr}$), band gap ($E_g$) and average size ($2R$) of ZnS nanoparticles prepared in various conditions

| No. | Stabilizer (S) | [S] | $\lambda_{tr}$, nm | $E_g$,Ev | 2R,nm |
|---|---|---|---|---|---|
| 1 | – | – | 345 | 3.62 | - |
| 2 | PVA | 2.5 mass % | 342 | 3.65 | 12.0 |
| 3 | Gelatine | 0.1 mass % | 326 | 3.83 | 5.6 |
| 4 | Gelatine | 2.0 mass % | 305 | 4.10 | 3.8 |
| 5 | CPC | $1{\cdot}10^{-3}$ M | 330 | 3.79 | 6.2 |
| 6 | SDS | $5{\cdot}10^{-3}$ M | 328 | 3.81 | 6.0 |
| 7 | SDS [a] | $5{\cdot}10^{-3}$ M | 313 | 4.0 | 4.4 |
| 8 | SDS [b] | $5{\cdot}10^{-3}$ M | 340 | 3.68 | 9.6 |
| 9 | SPPh | $5{\cdot}10^{-4}$ M | 303 | 4.10 | 3.8 |
| 10 | SPPh | $1{\cdot}10^{-3}$ M | 295 | 4.23 | 3.4 |
| 11 | SPPh | $5{\cdot}10^{-3}$ M | 313 | 4.0 | 4.4 |
| 12 | SPPh | $1{\cdot}10^{-2}$ M | 319 | 3.92 | 4.8 |
| 13 | Zn(II) | $5{\cdot}10^{-4}$ M | 313 | 4.00 | 4.4 |
| 14 | Zn(II) | $1{\cdot}10^{-3}$ M | 305 | 4.10 | 3.8 |
| 15 | Zn(II) | $2{\cdot}10^{-3}$ M | 301 | 4.15 | 3.6 |
| 16 | Zn(II)[c] | $2{\cdot}10^{-3}$ M | 291 | 4.30 | 3.2 |

[a] [ZnS] = $1{\cdot}10^{-4}$ M, [b] [ZnS] = $4{\cdot}10^{-3}$ M, in other cases [ZnS] = $1{\cdot}10^{-3}$ M. [c] Colloidal ZnS solution has been prepared via the addition of $Na_2S$ solution to the solution, containing an excess of Zn(II) over the stoichiometric amount, in other cases Zn(II) solutions have been added into the $Na_2S$ solutions.

$$\ln\alpha = \beta\frac{h\nu}{kT}(\text{at } h\nu < E_g)$$

where $\beta$ is a coefficient, $k$ is the Boltzmann constant.

*Effects of the synthesis conditions on the size of ZnS nanoparticles*

Figure 3 and Table 1 illustrate respectively absorption spectra and some optical characteristics of colloidal ZnS solutions, synthesized in various conditions. The band gap of ZnS nanocrystals, synthesized in the absence of stabilizers (Table 1, sample 1) is close to $E_g^{bulk}$. Such colloidal solutions are unstable and coagulate in 5–10 min after the preparation. Zinc sulfide nanoparticles with $E_g > E_g^{bulk}$, retaining prolonged stability toward the aggregation, can be obtained only in the presence of polymers (gelatine, PVA), cationic and anionic surfactants or an excess of Zn(II) (Table 1, samples 2–16). Maximal $E_g$ increase relatively to $E_g^{bulk}$ is 0.7 eV (Table 1, sample 16). It has been found that $E_g$ of ZnS nanocrystals, i.e., their size, can be tailored via the variation of the synthesis conditions (stabilizer and ZnS concentrations, order of reagents mixing and the viscosity of the dispersive medium, etc.).

*Stabilizer concentration*

Figure 3a illustrates the absorption spectra of colloidal ZnS solutions, synthesized in the absence of any stabilizer (curve 1) and in the presence of SPPh of different concentrations (curves 2–5 and Table 1, samples 9–12). Increase in SPPh concentration up to $2{\cdot}10^{-3}$ M results in the growth of the band gap of zinc sulfide nanoparticles to 4.23 eV and some $E_g$ decrease at larger stabilizer content. Aggregation stability of ZnS nanoparticles decreases symbately with $E_g$ diminution. Band gap decrement of ZnS nanoparticles at [SPPh] > $2{\cdot}10^{-3}$ M originates apparently from an increase in the ionic strength of the solution, forcing enlargement and coagulation of the nanocrystals. Growth of the band gap of ZnS nanoparticles in the presence of excessive Zn(II) represents another way of the influence on the size of ZnS nanocrystals (Table 1, samples 13–16). These results exemplify also the effect of the alteration of reagents mixing order on the size of ZnS nanoparticles (compare samples 15 and 16 in Table 1).

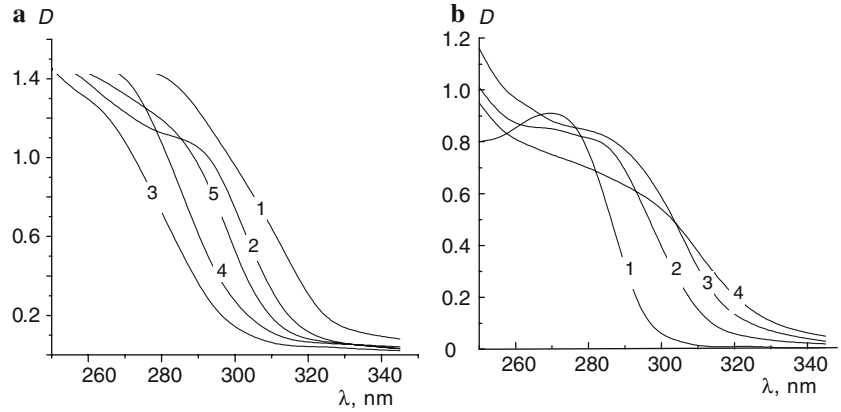


*Figure 3*. (a) Absorption spectra of non-stabilized ZnS colloid (1) and that of the colloids, synthesized in $5\cdot 10^{-4}$ M (2), $2\cdot 10^{-3}$ M (3), $1\cdot 10^{-2}$ M (4) & $3\cdot 10^{-2}$ M (5) solution of SPPh. [ZnS] = $1\cdot 10^{-3}$ M, $d$ = 1.0 cm. (b) Absorption spectra of colloidal ZnS solutions, synthesized in water, glycerol and water–glycerol mixtures. Volume ratio of water/glycerol mixtures is 0:10 (1), 3:7 (2), 5:5 (3) and 10:0 (4). [ZnS] = $2\cdot 10^{-3}$ M, $d$ = 0.2 cm.

*Dispersive medium viscosity*

It is known that the size of the precipitating crystallites of a poorly soluble substance is determined predominantly by the ratio of the rates of the nucleation and the nuclei growth. So, an increase in the medium viscosity, inhibiting the latter process, should result in a decrease in the size of forming ZnS nanocrystals. It has been actually found that the growth of the viscosity of water-glycerol mixtures with different components ratio is accompanied by the hypsochromic shift of $\lambda_{tr}$(Figure 3b) and the increase in the semiconductor band gap, indicating the diminution of the size of ZnS nanoparticles.

*ZnS concentration*

On the other hand, an increase in the concentration of colloidal solution, favoring to the growth of primary nuclei should result in the enlargement of forming nanocrystals. In accordance with this, at the increment of ZnS concentration from $1\cdot 10^{-4}$ to $4\cdot 10^{-3}$ M, the size of ZnS nanocrystals increases more than twice – from 4.4 to 9.6 nm (compare samples 7 and 8 in the Table 1).

*Photocatalytic Zn(II) reduction with the participation of ZnS nanoparticles*

No changes in the electronic spectra can be observed at the irradiation of colloidal ZnS solutions with the average particles size from 3.2 to 7.0 nm in the presence of only sodium sulfite. It can be concluded from this, that ZnS nanoparticles do not undergo cathodic photocorrosion in such conditions. On the other hand, gradual growth of the optical density over the whole investigated spectral domain can be observed (Figure 4) at the irradiation of these solutions in

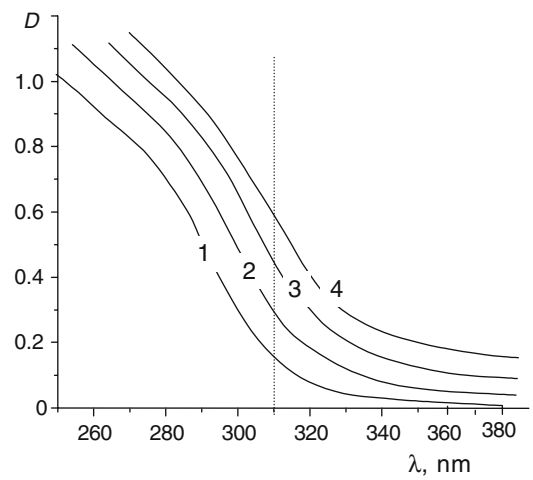


*Figure 4*. Absorption spectra of colloidal ZnS solutions, stabilized with SPPh and containing $ZnCl_2$ and $Na_2SO_3$, before the irradiation (1) and after the exposition for 15 (2), 30 (3) and 50 min (4). [ZnS] = $1\cdot 10^{-3}$ M, [SPPh] = $2\cdot 10^{-3}$ M, [$Na_2SO_3$] = $1\cdot 10^{-2}$ M, [$ZnCl_2$] = $2\cdot 10^{-3}$ M, pH 9.8.

the presence of both Zn(II) and $Na_2SO_3$. At that, originally colorless solutions become gray-brown.

The photoproduct has been found to be highly reactive toward the oxidants. Admission of the air to the irradiated cuvettes results in fast decoloration of the solutions, while the addition of the methylviologen (*N*,*N*-dimethylbipyridyl chloride, $MV^{2+}$) gives the product of one-electron reduction of $MV^{2+}$ – cation-radical $MV^{\bullet+}$, having characteristic absorption maximum at 605 nm and molar exctinction coefficient $\varepsilon_{605} = 13700\ M^{-1}\cdot cm^{-1}$ (Ramsden & Grätzel, 1984). These phenomena can be easily understood, if we assume that metallic zinc, $Zn^0$, is formed at the photochemical reduction of Zn(II) by sodium sulfite, induced by ZnS nanocrystals.

Formation of $Zn(OH)_2$ in the solutions of water-soluble zinc(II) salts begins already at pH 4–7. So, in centimolar sodium sulfite solutions $Zn^{2+}$ exist predominantly in the form of zinc(II) complexes of various composition with water and $OH^-$. These complexes are known to strongly adsorb to the surface of ZnS nanoparticles (Yanagida et al., 1990), determining their aggregation stability. It can be therefore concluded that photocatalytic Zn(II) reduction should take place on the surface of ZnS nanocrystals. It is apparently strong adsorption of Zn(II) complexes on the surface of ZnS nanoparticles that determines the constancy of the rate of photocatalytic reduction, observed in a wide range of Zn(II) concentrations ($5\cdot10^{-4}$–$4\cdot10^{-3}$ M).

The sole spectral change induced by the accumulation of the photoproduct consists in the growth of the optical density of the irradiated solutions over the whole measured spectral domain (Figure 4). So, we have used the optical density of a solution on arbitrarily chosed wave length $\lambda$ = 310 nm ($D_{310}$, dashed line in the Figure 4) for quantitative description of the kinetics of Zn(II) photoreduction. The molar $Zn^0$ exctinction coefficient at $\lambda$ = 310 nm, $\varepsilon_{310} = (1.1 \pm 0.1)\cdot\ 10^4\ M^{-1}\cdot\ cm^{-1}$, has been determined from the concentration of cation-radical $MV^{\bullet+}$, forming at the interaction between the photodeposited zinc and $MV^{2+}$. Using this $\varepsilon_{310}$ value we have determined the rates ($V_{Zn}$) and quantum yields of Zn(II) photoreduction ($\gamma_{Zn}$) in various conditions (refer to Figure 5 and Table 2).

The photoreaction rate grows at an increase in the excitatory light intensity (Figure 5a, curve 1). The rate $V_{Zn}$ has been found to depend upon the square of normalized light intensity $(I/I_0)^2$ (Figure 5a, curve 2). It is known that dependences of this sort are typical for two-electron photochemical reactions (Yanagida et al., 1989, 1990; Shiragami et al., 1993). So, we have concluded that the mechanism of photocatalytic Zn(II) reduction on the surface of ZnS nanoparticles includes a two-electron step.

It has been found that the photoreaction rate grows at a decrease in the size of semiconductor nanocrystals (Figure 5b). Taking into consideration that (i) high affinity of Zn(II) complexes to ZnS nanoparticles results in constant saturation

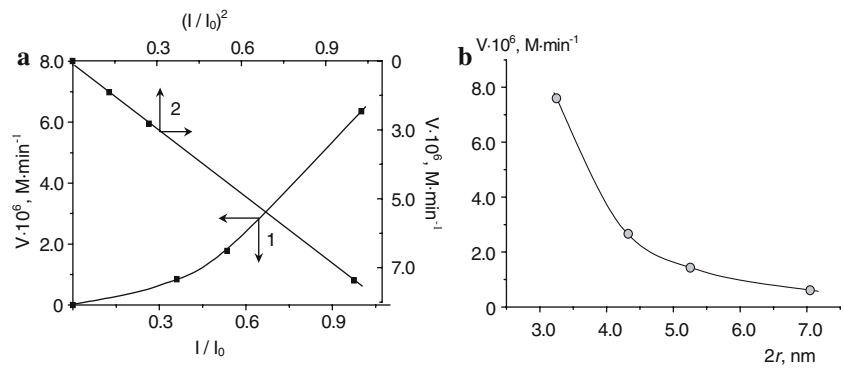


*Figure 5*. (a) Dependence between the rate of the photocatalytic Zn(II) reduction, $V_{Zn}$, and normalized light intensity $I/I_0$ (1) and the anamorphosis of this dependence in the coordinates $V_{Zn}$–$(I/I_0)^2$. (b) Correlation between the rate of Zn(II) photoreduction and the size of ZnS nanocrystals (2*R*). [ZnS] = $1\cdot\ 10^{-3}$ M, [SPPh] = $2\cdot\ 10^{-3}$ M, [$Na_2SO_3$] = $1\cdot\ 10^{-2}$ M, [$ZnCl_2$] = $2\cdot\ 10^{-3}$ M, pH 9.8.

*Table 2*. Quantum yields of the photocatalytic Zn(II) reduction

| No. | $[Na_2SO_3]\cdot 10^2$, M | pH | $\gamma_{Zn}\cdot 10^2$ |
|---|---|---|---|
| 1 | 0.2 | 9.6 | 1.8 |
| 2 | 0.4 | 9.6 | 2.9 |
| 3 | 0.8 | 9.6 | 4.7 |
| 4 | 2.0 | 9.6 | 8.7 |
| 5 | 2.0 | 8.4 | 4.6 |
| 6 | 2.0 | 9.0 | 5.9 |
| 7 | 2.0 | 9.8 | 8.8 |
| 8 | 2.0 | 10.6 | 4.6 |
| 9 | 2.0 | 11.4 | 2.3 |

*Notes:* $[ZnS] = 1\cdot 10^{-3}$ M, $[SPPh] = 2\cdot 10^{-3}$ M , $[ZnCl_2] = 2\cdot 10^{-3}$ M.

of the surface layer of the nanocrystals with Zn(II) and (ii) light absorption by ZnS nanocrystals of different size was complete in the conditions of our experiments, we have concluded that the correlation between the photoreaction rate and ZnS nanoparticles size originates from the size-dependent variation of the energy of photogenerated charge carriers. Our estimations have shown that the intensification of the spacial exciton confinement at the decrease of ZnS nanocrystals size from 7.0 to 3.2 nm results in the shift of ZnS conduction band potential $E_{CB}$ from −1.84 to −2.16 V *versus* NHE. Increment in the $E_{CB}$ potential results in turn, in the growth of the driving force of the photocatalytic reaction, which is thermodynamically possible even with the participation of bulk ZnS crystals (Roy & De, 2003).

It should be noted, however, that the increase in Zn(II) photoreduction rate at the diminution of the size of ZnS nanoparticles can arise not only from the augmentation of $E_{CB}$ modulus, but also from the changes of other properties of the photocatalyst, as well as conditions of the photoprocess – the diffusion rate of photogenerated charge carriers to the surface of ZnS nanocrystals of various size, the concentration of surface defects – traps of non-equilibrium charge carriers, the nature of adsorbed Zn(II) complexes, the aggregation rate of zinc atoms into $Zn^0$ nanoparticles on the surface of ZnS nanocrystals of different size, etc. It is apparently a combination of these factors that determines the gross dependence between the rate of Zn(II) photoreduction and the size of ZnS nanoparticles.

Growth of the efficiency of the surface capture of photogenerated valence band holes and consequent suppression of the electron-hole recombination have been considered as the most probable reasons for the augmentation of the $\gamma_{Zn}$ at the increment in sodium sulfite concentration (Table 2, samples 1–4).

The correlation between the photoreaction rate and pH of reacting mixture has been found to be quite complex (Table 2, samples 5–9). Additional experiments have shown that similar dependences between the quantum yield of the photocatalytic reaction and pH of the reacting mixture are also observed in other reactions with the participation of ZnS nanoparticles, especially, in photocatalytic hydrogen evolution from aqueous solutions of sodium sulfite or sodium sulfide. In both cases the maximal quantum yield is achieved at 9.6–9.8 regardless of the nature of the electronodonor used ($Na_2SO_3$ or $Na_2S$). So, we may conclude that the extremal correlations between the $\gamma_{Zn}$ and pH of the reacting media are not determined by the nature of the substrate of this specific reaction, but by the inherent properties of the surface of ZnS nanocrystals. In partucular, the growth of the rate of Zn(II) photoreduction in the pH range 8.4–9.7 can originate from the shift of $E_{CB}$ of ZnS nanocrystals toward more negative values as a result of hydroxyl ions adsorption (Yanagida et al., 1989).

Estimations, based on Nernstian Eq. (5), have shown that the pH growth from 0 to 9.7 is accompanied with the augmentation of $E_{CB}$ of zinc sulfide nanocrystals (and therefore the driving force of photocatalytic transformations on their surface) by 0.57 V:

$$E_{CB}^{pH} = E_{CB}^{0} + 0.059 \cdot pH \qquad (5)$$

where $E_{CB}^{pH}$ and $E_{CB}^{0}$ are conduction band potentials of ZnS nanocrystals at given pH and pH 0 respectively. The fall of the photoreaction efficiency at pH > 9.7 can be induced by tight blockage of the surface of ZnS nanoparticles by $OH^-$, resulting in the lowering of surface concentration of $HSO_3^-$ and $SO_3^{2-}$ and consequent growth of the probability of interband recombination of photogenerated charge carriers.

The following scheme summarizes above-discussed experimental results:

$$ZnS + h\nu \Rightarrow ZnS(e^-_{CB} + h^+_{VB}) \quad (6)$$

$$e^-_{CB} + h^+_{VB} \Rightarrow h\nu_1^{lum} + \Delta H \quad (7)$$

$$h^+_{VB} + SO_3^{2-} \Rightarrow SO_3^{\bullet -} \quad (8)$$

$$2SO_3^{\bullet -} \Rightarrow S_2O_6^{2-} \quad (9)$$

$$e^-_{CB} + []_{surf} \Rightarrow e^-_{tr} \quad (10)$$

$$h^+_{VB} + e^-_{tr} \Rightarrow h\nu_2^{lum} + \Delta H + []_{surf} \quad (11)$$

$$2e^-_{tr} + Zn(II)_{ads} \Rightarrow Zn^0_{ads} \quad (12)$$

$$ZnS/(nZn^0_{ads}) \Rightarrow ZnS/Zn^0_n \quad (13)$$

Here, $e^-{}_{CB}$ and $h^+{}_{VB}$ are ZnS conduction band electron and valence band hole, $\Delta H$ is the heat. Steps (7–9) correspond to some of the possible reactions of photogenerated charge carriers – interband reconbination (7), oxidation of adsorbed $SO_3^{2-}$ ions by valence band holes and subsequent recombination of anion-radicals $SO_3^{\bullet -}$ (reactions (8) and (9)) and, finally, capture of conduction band electrons by surface traps $[]_{surf}$ (10). The term "surface traps" refers in this case to various surface defects of ZnS nanocrystals as well as adsorbed Zn(II) complexes (Yanagida et al., 1989, 1990). Trapped electrons $e^-{}_{tr}$ have at least two possible concurring ways of withdrawal. First of them, process (11), generates heat and luminescence with $h\nu_2^{lum} < h\nu_1^{lum}$ ("defect" or donor–acceptor luminescence (Ramsden & Grätzel, 1984; Yanagida et al., 1989, 1990)), while the second way leads to the product of two-electron Zn(II) reduction – $Zn^0{}_{ads}$ (reaction (12)) and subsequent formation of $Zn^0$ nanoparticles (process (13)).

*Photocatalytic $KAu(CN)_2$ reduction on the surface of ZnS nanocrystals*

The long-wave edge of the fundamental absorption band of ZnS nanoparticles synthesized at [ZnS] = $1{\cdot}10^{-3}$ M and [SPPh] = $5{\cdot}10^{-3}$ M is located at $\lambda_{tr}$ = 313–315 nm. This $\lambda_{tr}$ corresponds to the band gap $E_g$ = 4.00–3.96 eV and the size of ZnS nanocrystals $2R$ = 4.4–4.5 nm. Absorption spectra of colloidal ZnS solutions remain unaffected by the addition of $KAu(CN)_2$ and $Na_2SO_3$. Irradiation of such systems both in the presence of air oxygen and in deaerated solutions results in the growth of the absorbance in the visible section of the spectrum and formation of new absorption band at 500–650 nm (Figure 6a). Absorption bands of this sort are known to belong to metallic gold nanoparticles and to be a superposition of the absorption band of $5d \rightarrow 6s$ interband electronic transition, lowering monotonously to longer wave lengths, and surface plasmon resonance (SPR) band with the maximum at 500–600 nm (Henglein, 1993). Rise of the gold SPR band in the absorption spectra of irradiated solutions indicates that $KAu(CN)_2$ reduction and subsequent formation of $Au^0{}_n$ nanoparticles take place at the irradiation. Since this photoreaction is by an order of magnitude slower when carried out in the absence of ZnS

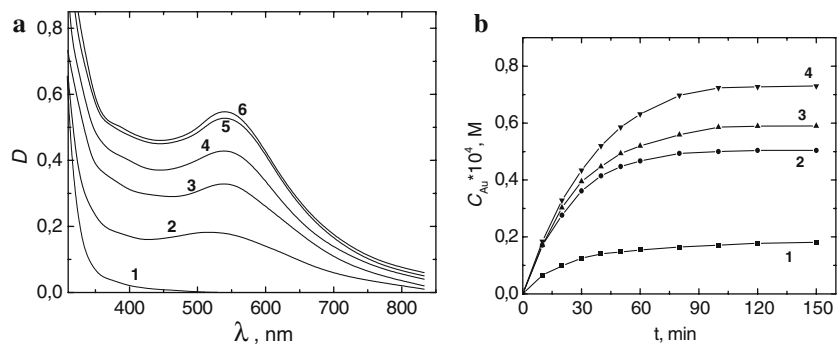


*Figure 6.* (a) Absorption spectra of air-saturated colloidal ZnS solution, containing $KAu(CN)_2$ and $Na_2SO_3$, before the irradiation (1) and after the exposition for 12 (2), 25 (3), 40 (4), 70 (5) and 95 min (6). [ZnS] = $5{\cdot}10^{-4}$ M. (b) Kinetic curves of gold accumulation at the irradiation of air-saturated colloidal ZnS solutions of different concentration in the presence of $KAu(CN)_2$ and $Na_2SO_3$. [ZnS] = $2{\cdot}10^{-4}$ (1), $5{\cdot}10^{-4}$ (2), $7{\cdot}10^{-4}$ (3) and $1{\cdot}10^{-3}$ M (4). [$KAu(CN)_2$] = $2{\cdot}10^{-4}$ M, [SPPh] = $5{\cdot}10^{-3}$ M, [$Na_2SO_3$] = $1{\cdot}10^{-2}$ M.

nanocrystals, we can conclude that semiconductor nanoparticles act as the photocatalyst, adsorbing complex ions $Au(CN)_2^-$ complex and catalyzing photochemical gold deposition at the expense of sulfite oxidation.

Ageing of the irradiated air-saturated solution in the dark results in gradual fall of the SPR band intensity. This observation indicates that the oxidation of $Au^0{}_n$ nanoparticles by air oxygen takes place in the systems under investigation, being possible apparently due to the presence of $CN^-$ ions.

Calculations, performed in the frames of Mie theory (Henglein, 1993), have shown that the maximum of gold SPR absorption band ($\lambda_m$) should be positioned at 520 nm in aqueous solutions. In accordance with these expectations, the maxima of SPR band of gold nanoparticles, formed at the photochemical (in the absence of ZnS nanoparticles) reduction of gold complex are located at $\lambda_m$ = 520–525 nm. Photocatalytic reduction of $KAu(CN)_2$ in the presence of ZnS nanocrystals, on the contrary, yields gold nanoparticles with $\lambda_m$ = 555–565 nm.

The most probable reason for the difference between the theoretically expected and experimental $\lambda_m$ positions of photocatalytically deposited gold consists, in our opinion, in the effect of the semiconductor on the electronic and optical properties of deposited $Au^0{}_n$ nanoparticles. It is natural to suppose that photoreduction of $KAu(CN)_2$ by ZnS conduction band electrons can efficiently compete with recombination processes only if this reaction takes place on the surface of ZnS nanocrystals. At that, gold nanoparticles are being formed on the interface of the two media with substantially different dielectric constants and refractive indices $n_0$ – aqueous solution ($n_0$ = 1.333) and zinc sulfide ($n_0$ = 2.367). Even rough estimations, performed with the average value $n_0' = \frac{1}{2}\cdot(1.333 + 2.367) = 1.850$ have given $\lambda_m$ = 555 nm, which is very close to the experimental $\lambda_m$ and confirmes our conjecture.

Absorption coefficient of highly dispersed metal $K(\lambda)$ can be calculated using the following expression (Henglein, 1993):

$$K(\lambda) = \frac{9\pi\eta n_0^3 c\lambda^2}{\sigma[(\lambda_m^2 - \lambda^2) + \lambda^2\omega^2]} \qquad (14)$$

where $\eta$ is the metal volume fraction, $\lambda$ is the wave length, $c$ is the light velocity in vacuo, $\omega$ is the FWHM of gold SPR band, $\sigma$ is the metal conductivity. The last parameter can be calculated from the equation (15).

$$\sigma = \frac{(\varepsilon_0 + 2n_0)c}{2\omega} \qquad (15)$$

where $\varepsilon_0$ is the wavelength-independent dielectric constant of the metal (for gold $\varepsilon_0$ = 9.9 (Antoine et al., 1997)).

Equation (14), transformed for the case $\lambda = \lambda_m$, can be used for the calculation of the metal volume fraction $\eta$ from two experimental parameters – $\omega$ and optical

$$\eta = 8.14 \cdot \frac{\sigma\omega^2 D_m}{n_0^3 c} \qquad (16)$$

density of SPR band in the maximum, $D_m$:

Values of $\eta$, calculated from the Eq. (16), have been then used for the determination of $Au^0$ concentration and the rate of the photocatalytic reaction.

Figure 6b illustrates kinetic curves of metallic gold accumulation at the irradiation of the solutions with $[KAu(CN)_2]$ = *const* and different ZnS concentrations. It can be seen from the figure that the photoreduction rate decreases gradually in the course of gold accumulation, the metal concentration achieving maximal value $C_{Au}^{max}$ and remaining virtally constant at further irradiation. When an additional amount of $KAu(CN)_2$ is added to the system, where maximal value $C_{Au}^{max}$ has settled, more metal can be photodeposited and new $C_{Au}^{max}$ achieved. So, ''plateaux'' on the kinetic curves of gold deposition are not associated with the irreversible inactivation of photocatalyst nanoparticles by photodeposited metal. On the other hand, resuming of the photoreaction after the addition of an extra amount of ZnS nanoparticles indicates that the ''plateaux'' on the kinetic curves do not originate from complete consumption of one of the reagents – $KAu(CN)_2$ or $Na_2SO_3$. To account for these facts, we supposed that the photocatalytic process under discussion is an equilibrium one, direct reaction of gold accumulation being the result of the interaction between photogenerated conduction band electrons ($e^-{}_{CB}$) and $Au(CN)_2^-$ anions, while reverse reaction being oxidation of deposited gold by ZnS valence band holes ($h^+{}_{VB}$). It has been mentioned above, that the presence of cyanide-ions, released in the course of

direct photocatalytic process, facilitates the oxidation of $Au^0_n$ nanoparticles by oxygen with the regeneration of $Au(CN)_2^-$. Since the standart potential $E^0(Au(CN)_2^-/Au^0) = -0.4$ V, we may suppose that ZnS valence band holes, having much more positive potential than oxygen, ($E(O_2/O_2^{\bullet -}) = -0.33$ V (Faust et al., 1989), are also capable of oxidizing gold nanoparticles.

In our experiments sodium sulfite concentration was of two orders of magnitude greater than the concentration of $KAu(CN)_2$ and 3–4 orders of magnitude higher than that of photodeposited metal. In such conditions kinetics of gold accumulation can be described by a formal kinetic equation for reversible first-order reactions:

$$C_{Au} = C^{max}_{Au}.(1 - e^{-(k+k')t}) \quad (17)$$

where $k$ and $k^/$ are the rate constants of direct and reverse reactions.

Equation (17) can be transformed as follows:

$$\lg(C^{max}_{Au} - C_{Au}) = \lg C^{max}_{Au} - 0.434(k + k')t \quad (18)$$

It has been found that the kinetic curves of gold photodeposition are actually linear in the coordinates $\lg(C^{max}_{Au} - C_{Au}) - t$, confirming in that way our conjecture about the equilibrium nature of the photocatalytic process. The constants sum $k + k^/$, which has been calculated as the slope ratio of linearized kinetic curves (Table 3), decreases at an increment in ZnS concentration. So, one of the constants (or both of them) has to be an effective value.

From $C^{max}_{Au}$ we have determined the equilibrium constant of the photoreaction $K_e$ as well as the constants of direct and reverse reactions:

$$K_e = \frac{C^0_{Au} - C^{max}_{Au}}{C^{max}_{Au}} = \frac{K_e}{1 + K_e}(k + k') \quad k' = \frac{k + k'}{1 + K_e} \quad (19)$$

Calculations, based on the Eqs. (19) for the systems with different ZnS content (Table 3), have shown that $k^/$ remains virtually constant at an increase in ZnS concentration, while $k$ decreases in such conditions. The reason of $k$ lowering may consists, in our opinion, in adsorption equilibrium shift at a change in $[ZnS]/[KAu(CN)_2]$ ratio, which has not been taken into account by formal kinetic equations (17–19). Correlation between the rate of gold accumulation, $V_{Au}$, and the initial concentration of $KAu(CN)_2$ (Figure 7a, curve 1) has been found to be linear in the Langmuirian coordinates $V^{-1}_{Au} - [KAu(CN)_2]^{-1}$ (Figure 7a, curve 2), indicating that it is the gold complex, adsorbed on the surface of ZnS nanocrystals, that participates in the photocatalytic reaction. Growth of the ratio $[ZnS]/[KAu(CN)_2]$ at an increase in ZnS concentration and $[KAu(CN)_2] = const$ results in the depletion of the surface layer of ZnS nanoparticles with $Au(CN)_2^-$ anions and subsequent decrease of the effective rate constant of the direct photoreaction. Inlinearity of the dependence between the rate of the photocatalytic reaction and ZnS concentration at $[ZnS] > 7\cdot 10^{-4}$ M (Figure 7b) has apparently the same origin.

We propose the following mechanism of the photocatalytic $KAu(CN)_2$ reduction with the participation of ZnS nanoparticles:

$$Au(CN)_2^- + []_{ads} \Rightarrow Au(CN)^-_{2\,ads} \quad (20)$$

$$HSO_3^- + []_{ads} \Rightarrow HSO^-_{3\,ads} \quad (21)$$

$$ZnS + h\nu \Rightarrow e^-_{CB} + h^+_{VB} \quad (22)$$

$$e^-_{CB} + Au(CN)^-_{2\,ads} \Rightarrow Au^0_{ads} + 2CN^- \quad (23)$$

$$h^+_{VB} + HSO^-_{3\,ads} \Rightarrow HSO^{\bullet}_{3\,ads} \quad (24)$$

$$nAu^0_{ads} \Rightarrow Au_n \quad (25)$$

$$h^+_{VB} + Au_n + 2CN^- \Rightarrow Au_{n-1} + Au(CN)_2^- \quad (26)$$

where $[]_{ads}$ is the adsorption site on the surface of ZnS nanocrystals.

*Table 3*. Kinetic parameters of the photocatalytic $Au(CN)_2^-$ reduction.

| No. | $[ZnS]\cdot 10^4$, M | $C^{max}_{Au}\cdot 10^5$, M | $K_e$ | $k + k^/, \cdot 10^4$, $s^{-1}$ | $k\cdot 10^4$, $s^{-1}$ | $k^/\cdot 10^5$, $s^{-1}$ |
|---|---|---|---|---|---|---|
| 1 | 5.0 | 5.1 | 2.9 | 3.2 | 2.4 | 8.2 |
| 2 | 7.0 | 6.2 | 2.2 | 2.7 | 1.9 | 8.5 |
| 3 | 10.0 | 7.5 | 1.7 | 2.4 | 1.5 | 8.6 |

*Notes*: $[KAu(CN)_2] = 2\cdot 10^{-4}$ M, $[SPPh] = 5\cdot 10^{-3}$ M, $[Na_2SO_3] = 1\cdot 10^{-2}$ M.

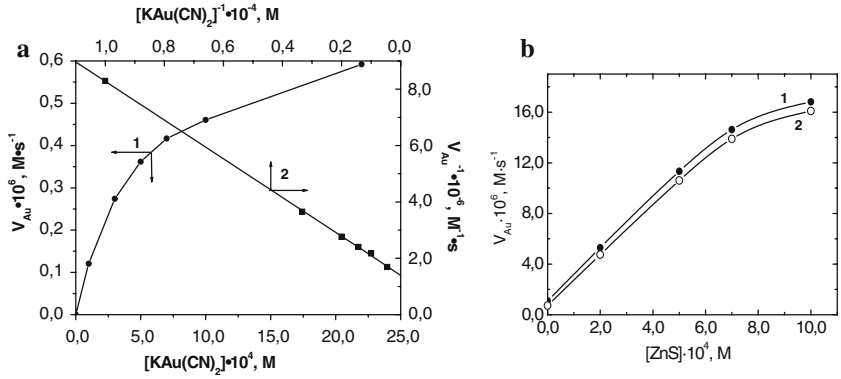


*Figure 7.* (a) Dependence between the rate of the photocatalytic gold deposition and initial concentration of $KAu(CN)_2$ (1) and the anamorphosis of this dependence in the coordinates $V_{Au}^{-1}$– $[KAu(CN)_2]^{-1}$ (2). (b) Dependence between the rate of the $KAu(CN)_2$ photoreduction in deaerated (1) and air-saturated (2) solutions and molar ZnS concentration. ZnS colloids of different concentration have been prepared from the stock solution of [ZnS] = $1{\cdot}10^{-3}$ M. $[KAu(CN)_2]$ = $2{\cdot}\ 10^{-4}$ M, [SPPh] = $5{\cdot}\ 10^{-3}$ M, $[Na_2SO_3]$ = $1{\cdot}\ 10^{-2}$ M.

Here, the processes (20) and (21) correspond to the adsorption of the reactants on the surface of ZnS nanoparticles, step (22) is the photogeneration of charge carriers, reactions (23) and (24) are the reduction of adsorbed $Au(CN)_2^-$ and oxidation of adsorbed $HSO_3^-$ respectively. $HSO_3^{\bullet}$ radicals can further dimerize in deaerated solution or interact with the oxygen in air-saturated media (Faust et al., 1989). Processes (25) and (26) correspond to the aggregation of atomic gold and oxidation of $Au^0{}_n$ nanoparticles by ZnS valence band holes respectively.

## Conclusions

In the present paper we have discussed spectral properties and the structure of the long-wave edge of the fundamental absorption bands of ZnS nanoparticles of different size. Effects of the synthesis conditions upon the size and optical properties of ZnS nanoparticles, stabilized in aqueous solutions, have been analyzed.

We have investigated the photochemical Zn(II) reduction by sodium sulfite, catalyzed by ZnS nanocrystals. It has been shown that the increment in the modulus of ZnS conduction band potential, induced by the reinforcement of spacial exciton confinement at the decrease in the size of semiconductor nanoparticles, results in the growth of the rate of this photocatalytic process. The mechanism of Zn(II) photoreduction has been found to involve the step of two-electron reduction of complex Zn(II) forms, adsorbed on the surface of ZnS nanocrystals.

Photocatalytic activity of ZnS nanocrystals in $KAu(CN)_2$ reduction in aqueous solutions of sodium sulfite has been found. Kinetics of this process as well as the spectral characteristics of forming ZnS/Au nanocomposite have been investigated. It has been concluded that photocatalytic $KAu(CN)_2$ reduction is the equilibrium process due to the reverse oxidation of gold nanoparticles by ZnS valence band holes.

## References

Antoine R., P.F. Brevet & H.H. Girault et al., 1997. Surface plasmon enhanced non-linear optical response of gold nanoparticles at the air/toluene interface. Chem. Commun. 1901.

Dhas N.A., A. Zaban & A. Gedanken, 1999. Surface synthesis of zinc sulfide nanoparticles on silica microspheres: Sonochemical prerparation, characterization, and optical properties. Chem. Mater. 11, 806–813.

van Dijken A., A.H. Janssen, M.H. Smitsmans, et al., 1998. Size-selective photo-etching of nanocrystalline semiconductor nanoparticles. Chem. Mater. 10, 3513–3522.

Faust B.C., M.R. Hoffmann & D.W. Bahnemann, 1989. Photocatalytic oxidation of Sulfur Dioxide in Aqueous Suspensions of $\alpha$-$Fe_2O_3$. J. Phys. Chem. 93, 6371–6381.

Gaponenko S.V., 1996 Optical Properties of Semiconductor Nanocrystals. Cambridge: University Press.

Grätzel M. ed., 1983. Energy Resources through Photochemistry and Catalysis. Academic Press, New York, USA.

Henglein A., 1993. Physicochemical properties of small metal particles in solution: ''Microelectrode'' reactions, chemisorption, composite metal particles, and the atom-to-metal transition. J. Phys. Chem. 97, 5457–5471.

Kanemoto M., T. Shiragami, C. Pac & S. Yanagida, 1992. Semiconductor photo-catalysis. Effective photoreduction of carbon dioxide catalyzed by ZnS quantum crystallites with low density of surface defects. J. Phys. Chem. 96, 3521–3526.

Kanemoto M., H. Hosokawa, Y. Wada, et al., 1996. Semiconductor photocatalysis. Part 20. Role of surface in the photoreduction of carbon dioxide catalyzed by colloidal ZnS nanocrystallites in organic solvents. J. Chem. Soc., Faraday Trans. 92, 2401–2411.

Korzhak A.B., N.I. Ermokhina & A.L. Stroyuk et al., 2005. Photocatalytic activity of mesoporous $TiO_2$/Ni composite in hydrogen evolution from aqueous-alcoholic mixtures. Theoret. Experim. Chem. 41, 24–29.

Kryukov A.I, S.Y. Kuchmii & V.D. Pokhodenko, 2000. Energetics of the electronic processes in semiconductor photocatalytic systems. Theoret. Experim. Chem. 36, 69–88.

Nanda J., S. Sapra & D.D. Sarma, 2000. Size-selected zinc sulfide nanocrystallites: Synthesis, structure, and optical studies. Chem. Mater. 12, 1018–1024.

Ramsden J.J. & M. Grätzel, 1984. Photoluminescence of small cadmium sulphide particles. J. Chem. Soc., Faraday Trans. 1(80), 919–933.

Roy A.M. & G.C. De, 2003. Immobilization of ZnS, CdS and mixed ZnS-CdS on filter paper. Effect of hydrogen production from alkaline $Na_2S/Na_2S_2O_3$ solution. J. Photochem. Photobiol. A: Chem 157, 87–92.

Shiragami T., H. Ankyu, S. Fykami, et al., 1992. Semiconductor photocatalysis: Visible light induced photoreduction of aromatic ketones and electron-deficient alkenes catalysed by quantized cadmium sulfide. J. Chem. Soc. Faraday Trans. 88, 1055–1061.

Shiragami T., S. Fukami, Y. Wada & S. Yanagida, 1993. Semiconductor photocatalysis. Effect of light intensity on nanoscale CdS-catalyzed photolysis of organic substrates. J. Phys. Chem. 97, 12882–12887.

Stroyuk A.L, A.V. Korzhak, A.E. Raevskaya, et al., 2004. Photocatalysis of hydrogen evolution from aqueous sodium sulfitre solutions by composite CdS/Ni nanoparticles. Theoret. Experim. Chem. 40, 1–6.

Stroyuk A.L., V.V. Shvalagin & S.Y. Kuchmii, 2005. Photochemical synthesis and optical properties of binary and ternary metal-semiconductor composites based on zinc oxide nanoparticles. J. Photochem. Photobiol. A.: Chem. 173, 185–194.

Tada H., T. Ishida, A. Takao, et al., 2005. Kinetic and DFT studies on the Ag/$TiO_2$-photocatalyzed selective reduction of nitrobenzene to aniline. Chem. Phys. Chem. 6, 1537–1543.

Yanagida S., M. Yoshiya, T. Shiragami, et al., 1990. Semiconductor photocatalysis. Quantitative photoreduction of aliphatic ketones to alcohols using defect-free ZnS quantum crystallites. J. Phys. Chem. 94, 3104–3111.

Yanagida S., Y. Ishimaru, Y. Miyake, et al., 1989. Semiconductor photocatalysis. ZnS-catalyzed photoreduction of aldehydes and related derivatives: Two-electron-transfer reduction and relationship with spectroscopic properties. J. Phys. Chem. 93, 2576–2582.

Wang Y. & N. Herron, 1991. Nanometer-sized semiconductor clusters: Materials synthesis, quantum size effects and photophysical properties. J. Phys. Chem. 95, 525–532.

Zhang H., F. Huang, B. Gilbert & J.F. Banfield, 2003. Molecular dynamics simulations, thermodynamic analysis, and experimental study of phase stability of zinc sulfide nanoparticles. J. Phys. Chem. B 107, 13051–13060.